Available online at www.sciencedirect.com
SCIENCE DIRECT®
Thermochimica Acta 411 (2004) 125–131
thermochimica acta
www.elsevier.com/locate/tca

Measurement of intrinsic material damping using differential calorimetry on specimens under uniaxial tension

J. Åberg*, B. Widell, T. Bergström, H. Fredriksson

KTH, Casting of Metals, Brinellvägen 23, Stockholm S-100 44, Sweden

Received 23 July 2003; accepted 11 August 2003

Abstract

A method has been developed to measure the intrinsic damping capacity of metals. A specimen is subjected to a cyclic uniaxial stress, to give a prescribed energy input. The amount of energy that is stored in the specimen is measured using differential calorimetry, i.e. the difference in temperature between the specimen under stress and a non-stressed reference sample is measured. The experiments were performed in an insulated vacuum container to reduce convective losses. The heating rate, together with the energy input, is used as a measure of the intrinsic material damping in the specimen. The method has been developed by testing an aluminium based and a stainless steel alloy. It is possible to distinguish the difference in damping between these two alloys.

Keywords: Intrinsic; Damping; Calorimetric methods; Material properties

1. Introduction and background

It is important to take the intrinsic damping capacity property into consideration when designing new materials to ensure that they fulfil traditional specifications as well as having good damping properties.

The intrinsic damping capacity is one of a number of parameters that should be taken into account when designing the product. The damping property should be stated in tables in the same way as other material properties such as Young's modulus, creep curves, yield stress, hardness, density, thermal conductivity and thermal capacity.

The concept intrinsic damping capacity is used to mean something that might be called specific intrinsic material damping, an intensive, mass independent quantity, see for instance Kinra and Yapura [1]. Damping can be considered as consisting of three types of phenomena. Firstly, damping due to the way the component is fastened to its surroundings; a component fastened with many rivets and bolts will be damped by energy loss in the connectors. Secondly, some shapes give better damping than others, and finally, the intrinsic damping capacity, the way the vibration energy is transformed into other forms of energy within the material itself.

To design materials with good damping properties it is necessary to understand the interaction between the intrinsic damping capacity and design parameters of the material such as internal structure and the manufacturing parameters controlling the structure. A large number of mechanisms affect the dissipation of vibration energy within a material. Most of the published information about these mechanisms is of an empirical nature, and the underlying physical nature is not fully understood [2]. Therefore, knowledge about the influence of different material design parameters such as chemical composition, melt treatment, solidification speed, microstructure and heat treatment on the damping properties has not yet been fully investigated and understood. Empirically, it is known that some cast materials have better damping properties than others. One such material is grey cast iron, where it is believed that the morphology of its graphite affects the damping properties. Usoltsev [3] found that the relative intrinsic damping capacity of a spheroidal graphite structure is half that of a vermicular, whereas a lamellar structure has an intrinsic damping capacity which is four times better than the vermicular. Damping is associated with all types of materials. Many attempts have been made to understand its nature but it still remains a poorly understood phenomenon. According to Spence and Kenchington [4], it is not an overstatement to say that the intrinsic damping capacity cannot be predicted or modelled

* Corresponding author. Tel.: +468-7906151; fax: +468-216557.
E-mail address: jonasa@matpr.kth.se (J. Åberg).

0040-6031/$ – see front matter © 2003 Elsevier B.V. All rights reserved.
doi:10.1016/j.tca.2003.08.011

Nomenclature

c_p	specific heat capacity (J/K kg)
E	modulus of elasticity (N/m^2)
f	frequency (s^{-1})
F	force (N)
L	length (m)
m	mass (kg)
s	displacement (m)
T	temperature (K)
W	work (Nm)
$\dot{W}$	power (Nm/s)

Greek letters

ε	strain
η	loss factor
ρ	density (kg/m^3)
σ	stress (N/m^2)

with any degree of accuracy. To date it can only be derived as an average of a large number of measurements.

It is necessary to measure the intrinsic damping capacity to be able to develop intrinsic damping capacity models. Existing methods can be put into two groups, i.e. analysis of the effect the test material has on an input signal using Fourier analysis [5] and the measurement of the decay in the amplitude of a vibrating test piece [6]. There are problems with both methods, they either assume a linear equation of motion for the material tested, only giving information at certain frequencies depending on which eigen frequencies the test piece has or they measure the damping with a load that is not uniaxial. An example of measurements using Fourier analysis is presented in [7] where a number of materials were tested. The method was found to be unsuitable for a number of reasons, such as the geometry of the test pieces, the dissipation of energy into the surrounding air, simplification due to the assumption of a linear model for the material damping, the use of a single degree of freedom model on a multiple degree of freedom system and possible losses due to the method for fastening of the test pieces to their surroundings. A further limitation of the method is that only a very small range of linear behaviour can be tested and that the dependence of the strain level on the material damping cannot be tested. An alternative would be to measure the difference between stress and strain in a cyclic sinusoidal motion. This has been investigated in [8,9] and refined in [10], but the method has limitations due to its complexity and its limited ability to measure low damping metals.

2. Methods

To circumvent the problems and questions regarding existing methods it was desirable to look for a method of a more fundamental nature, relating to the basics of damping, but avoiding the traditional way of building a mathematical model based on the equation of motion for the material. It was assumed that some of the vibration energy in a material is transferred to heat during the process of damping. The relation between the input of energy and heating is then a measure of the damping in the material. Initial calculations were performed to estimate the heating rate as a function of the input of mechanical energy. The basic idea is to impose the load during uniaxial testing. It is evenly distributed within the material without plastic deformation and all energy from damping is converted to heat and measured as a temperature increase. This temperature increase depends on the density, volume and specific heat of the material. It was also assumed that the loss of energy to the surroundings is negligible. The calculations indicate that it should be possible to measure the temperature increase due to the intrinsic internal damping if it is possible to ascertain that only small amounts of energy transfer takes place between the test piece and the surroundings.

Two bars are placed in a vacuum chamber. The *test bar* is in contact with the top and bottom of the vacuum chamber whilst the *reference bar* is suspended from a plastic hook in the ceiling, ensuring that it does not touch the measured bar or the walls of the test chamber. The temperature of the test bar as a function of time is measured differentially to the reference bar using thermocouples. The vacuum chamber is placed inside an MTS [11] tensile test machine with compression platens. The test bar will thus be cyclically stressed by compression. Two control and measurement systems are used, one to control and measure the load input, the other to measure the temperature increase.

2.1. Sub-systems

Fig. 1 illustrates the general sub-system assembly. It consists of a load input system in the form of a tensile test machine, a vacuum system to reduce convective heat transfer and a differential temperature measurement system consisting of two bars, thermocouples and a microvolt meter.

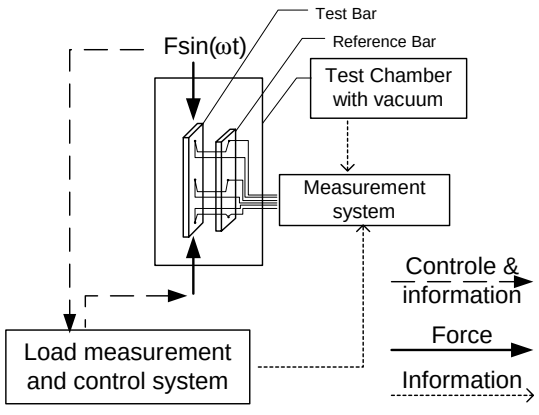

Fig. 1. Principal set-up.

2.2. Load input system

The system used to impose the compression load on the test bar is a conventional tensile test machine, an MTS 810 loadframe with an MTS Teststar controller and MTS Testware SX 4.0 to write the control code programs.

2.3. Temperature measurement system based on differential thermocouples

An accurate temperature measurement system is needed since the temperature increase is rather small, typically 10^{-4} °C/s. Temperature measurement using thermocouples is a way of measuring the temperature difference between a point of known temperature and one of unknown temperature. The temperature of the reference point is measured using an independent method. The most frequently used sensor technique for measurement of the reference temperature is the monolithic temperature sensor. This reference temperature measurement, in combination with a thermocouple usually gives the temperature with an accuracy of within 1 °C. Better accuracy can be achieved with a better reference temperature source such as an ice and water mixture. The ice pool temperature varies very little with air pressure. The problems with this technique are practical. The problem of measuring small temperature changes due to a specific parameter is different. If the temperature point measured is affected by several parameters, it is preferable to use a reference point, which has a temperature that varies in the same way except for the parameter dependency sought for. This was done by putting a reference bar together with the test bar under cyclic stress. Since the temperature difference between the test and reference bar is small, they are affected by conduction through the near vacuum, convection and radiation in the same way.

The choice of thermocouple was governed by two factors. The first was stable behaviour at room temperature and the second, a high and well-defined Seebeck coefficient, to increase the strength of the output signal. This gives well-defined material properties in the thermocouple wire, so that the material properties are independent of the longitudinal position in the wire, or put another way, the standard deviation of the Seebeck coefficient should be small.

The use of a thermopile was considered, but was decided against. A thermopile would physically extend along the bar. Hence, if there is a propagating thermal disturbance along the bar it would be included in the reading.

Type-T thermocouples, copper/constantan, with a Seebeck coefficient of about 40.3 μV/°C at 20 °C were used. The alternative was type-J, which has a 25% higher Seebeck coefficient but not as good standard deviation of its material properties [12]. The thermocouple wire was purchased on a roll. Type-T wire is blue (Cu) and red (constantan) according to ANSI MC 96.1 [13]. The red and blue wires were separated. The blue wire lead from the measurement instrument into the vacuum chamber. The tips of the two blue wires were interconnected using a red wire, each connection being a sensor. One was placed on the test bar, the other on the reference bar (Fig. 2).

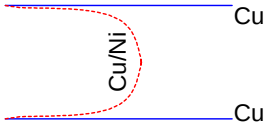

Fig. 2. Differential thermocouple.

The thermocouples were welded using a technique known under a variety of names, i.e. tungsten inert gas (TIG), wolfram inert gas (WIG), gas tungsten arc welding (GTAW) using a thin bar of tungsten surrounded by an inert gas. The two wires were held together, an arc was struck and the wires were put into the arc. After welding, the arc was turned off, but the inert gas remained on during solidification and cooling of the weld to prevent it from oxidising.

The Seebeck effect produces a potential difference due to the temperature difference. If the thermocouples were directly connected to the electrically conducting test and reference bar, it would affect the readings of all the sensors in electric contact with the system. To avoid this, the bars were coated with five thin layers of Electrolube Acrylic Protective Lacquer [14]. The number of layers needed were tested. The number of layers was decided after experiments indicated that if the layer was too thin the acrylic was sometimes penetrated by the thermocouple tip when a pressure load was applied to keep the thermocouple in place on the bar.

The thermocouple and the bar were covered with thermal conductivity paste to ensure a good thermal contact at the contact surface. In order to distribute the pressure, a piece of cardboard was fixed on top using a paper clip of just the right size.

Fig. 3 shows the mounting. The thermocouple wires, the cardboard and the paperclip can be seen. It is also possible to observe a hole in the upper part of the shorter reference bar, which is used to hang the bar in. The design of the hole and the hook means that the bar is unable to twist and minimises the risk for contact with the measurement bar or the walls of the vacuum chamber. To check the function of the thermocouples the tips on the sensors were put into a mixture of ice and pure water within 2 mm of each other. They showed a temperature difference between 0.02 and 0.1 K.

During the experiments the tabulated Seebeck coefficient at 20 °C was used. The electric signals from the thermocouples were fed directly into a Hewlett-Packard, HP34970A Digital multimeter using an internal HP34901A multiplexer [15]. The instruments were controlled from a PC using the HP Benchlink v1.3 software supplied with the instrument.

The test chamber is a tube with connectors to the vacuum system for the extraction of air, a dummy that is not used and a connector for all the thermocouples (Fig. 3). To minimise external electric interferences, all the thermocouples were

Fig. 3. The test bars and vacuum chamber.

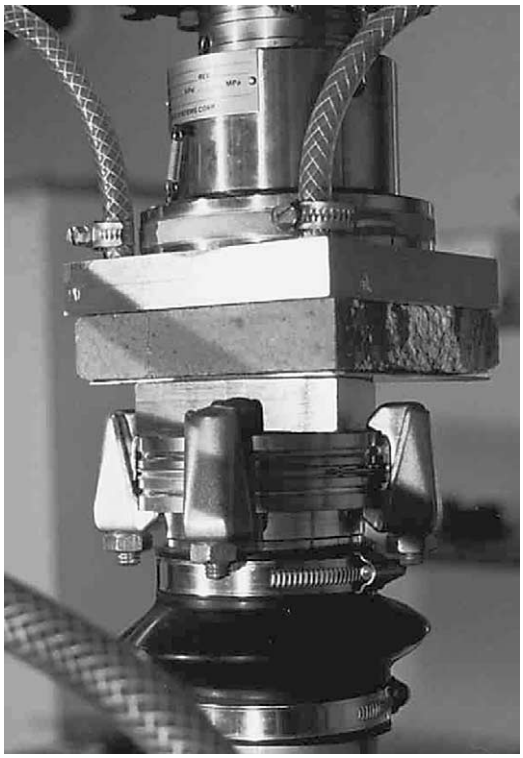

Fig. 4. Upper end of vacuum test chamber.

protected with a coaxial shield with common electric ground to the rest of the measurement system.

During initial testing, it was discovered that the MTS machine caused considerable thermal disturbance. After the initial period of time during which the test and reference bar were meant to come to thermal equilibrium, there was still an approximately linear temperature variation in the bar, a few degrees higher at the lower end than at the higher end. At the start of the experiment, the lower end of the bar was heated more than the upper end. This was due to the hydraulic actuator in the MTS machine. When the control system started the cyclic loading, heated oil at about 40 °C was fed via the control valve to the actuator, which in turn heated the test chamber and finally, the bar. This problem was solved by cooling the MTS pressure platens, and by using insulating blocks (Fig. 4). A water reservoir was put beside the MTS machine and its temperature was controlled via a thermostat and a solenoid valve effecting the flow of external cold water through a cooling coil in the reservoir. The reservoir water was transferred to the aluminium cooling plates using a centrifugal pump. Fig. 4 shows the arrangement of the equipment; at the top the pressure platen, then an aluminium block with internal cooling channels and the in- and outlet hoses. A ceramic block and a thin sheet of stainless steel are beneath to distribute the stress. Further down the end piece of the test chamber can be seen, different seals and clamps, and at the bottom there is a rubber seal that takes up the longitudinal strain in the test chamber to prevent it from absorbing any load.

To track the system and its surrounding the following parameters have been monitored: the temperature difference between nine evenly spaced points on the test bar and the absolute temperature in the room, the differential temperature between the reference bar and the vacuum chamber, the absolute temperature of the reference bar, the inlet and outlet water temperature to the cooling plates, the pressure in the vacuum chamber and the state of the MTS test machine. Not all of these were monitored during all the experiments, and some were abandoned after finding them to be of minor importance.

From the beginning it was feared that disturbances from the end of the bars would interfere with the measurements. It was thought that friction between the end of the bars and the endplates could produce heat that together with outside temperature changes could result in temperature gradients that propagate through the bar during the experiment. This would give an additional temperature increase, which could be misinterpreted as an increase in the intrinsic damping in the bar. To make a conservative estimate of the time it takes for an external disturbance to propagate from the end to the sensor in the middle of the test bar, the following method was used. The temperature of the cooling water of the cooling plates was raised by about 20°. The temperature versus time curves for the differential sensors were recorded.

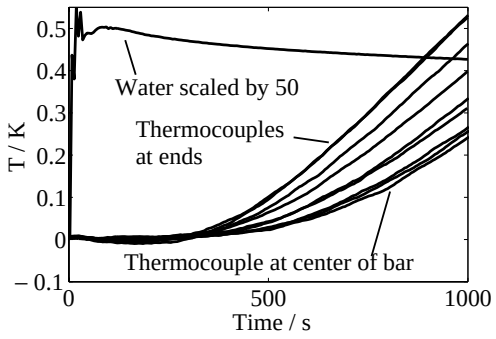

Fig. 5. Experimental temperature distribution.

It was concluded that it takes about 5 min before this external disturbance reaches the middle and affects the reading for an aluminium alloy (Fig. 5). This is a conservative estimate since the external heat source is considerably smaller during an experiment. For steels and cast iron, the undisturbed time is longer due to the lower diffusion rate of heat in these materials. The step function temperature in Fig. 5 is scaled down by a factor of 50.

3. Theory

During the experiments, various load amplitudes and frequencies were used for the different materials, depending on limitations in the test machine and bending of the test specimen. These parameters, as well as the material damping influence the temperature increase. It is necessary to derive an expression for the material damping in the system from the temperature–time gradient. The authors have chosen to use the loss factor [16], which for small values of damping is related to other definitions of damping through the following relationships according to [17]

$$Q^{-1} = \frac{\psi}{2\pi} = \eta = \frac{\delta}{\pi} = \tan\phi = \frac{E''}{E'} = 2\zeta = \frac{\Delta W}{2\pi W} \tag{1}$$

Q^{-1} is the quality factor, ψ the specific damping, η the loss factor, δ the logarithmic decrement, ϕ the loss angle, E' the storage modulus, E'' the loss modulus, ζ the damping ratio and W the energy fed into the system during a load cycle. An expression for the loss factor will be derived and the total input of mechanical energy will be compared with the energy dissipated within the bar. In this paper, is assumed that the stress is elastic and linked to the strain via the modulus of elasticity, $\sigma = \varepsilon E$, the strain is defined as

$$\varepsilon = \frac{s}{L} \tag{2}$$

where ε is the strain, s the displacement and L the length. The energy can be expressed as mechanical work.

$$W = \int F\,\mathrm{d}x \tag{3}$$

where W is the work, F the imposed force and x the room co-ordinate, or the energy could be expressed as heat

$$W = Tc_\mathrm{p}V\rho \tag{4}$$

where T is the temperature, c_p the heat capacity, V the volume and ρ the density. The loss factor is defined as

$$\eta = \frac{\Delta W}{2\pi W} \tag{5}$$

where ΔW in the nominator is the work transferred to heat during a load cycle and W in the denominator is the total mechanical elastic energy fed to the system during a load cycle.

The mechanical energy fed into the system per unit of time is given by Eq. (3) and multiplied with the frequency, f

$$\dot{W}_\mathrm{mechanical} = f\int_0^s F\,\mathrm{d}x = \left\{\mathrm{d}x = L\frac{\mathrm{d}F}{AE}\right\} = f\int_0^F \frac{FL}{AE}\mathrm{d}F = f\frac{F^2L}{2AE} \tag{6}$$

The energy transferred to heat per unit of time is given by exchanging the temperature, with its derivative in Eq. (4)

$$\dot{W}_\mathrm{heat} = \frac{\mathrm{d}T}{\mathrm{d}t}c_\mathrm{p}V\rho = \frac{\mathrm{d}T}{\mathrm{d}t}c_\mathrm{p}AL\rho \tag{7}$$

where $\mathrm{d}T/\mathrm{d}t$ is the heating rate, A the cross-sectional area and L the length of the bar.

Using the expression for the loss factor, Eq. (5), and inserting Eqs. (6) and (7) gives

$$\eta = \frac{(\mathrm{d}T/\mathrm{d}t)c_\mathrm{p}AL\rho}{2\pi f(F^2L/2AE)} = \frac{(\mathrm{d}T/\mathrm{d}t)c_\mathrm{p}A^2\rho E}{\pi f F^2} \tag{8}$$

The equation shows that for a certain material with known thermophysical properties, geometry and with known test parameters, the temperature–time derivative gives a value for the material damping.

4. Experiments

Before an experiment can begin the test chamber should be in the machine, parallel to the loadframe. A static load equal to the mean value of the power spectrum to be used is introduced. The rig is then left so that the test and reference bar can reach thermal equilibrium. The control program for the MTS and the thermal data logging are started. The program initially waits for 15 min to gather temperature readings for the state before the cyclic load is applied. One temperature-logging channel is used to indicate that the cyclic load is imposed on the test bar. The cyclic load is maintained for approximately 10 min. For repeated tests, the system rests at the mean load for typically 4 h before continuing with the next test. This automation by the control program makes more efficient testing possible as tests can run over night and the weekend.

The data was exported from the HP Benchlink and imported to Matlab [18]. In Matlab, the data from the thermocouple readings were plotted and analysed. Data from 100 readings per thermocouple channel just prior to commencing a test were used to calibrate the initial temperature reading to create a time independent temperature distribution plot at the start of the experiment. The temperature readings were then used to calculate the initial temperature–time derivative for the middle point of the test bar and draw temperature distribution plots for the test.

A number of experiments were performed. The results from tests on two different metals, a stainless steel and an aluminium alloy, will be presented in this paper.

The aluminium is a Swedish Standard SS4253, sandcast with 10% silicon and about 0.3% magnesium. The stainless steel is a Sandvik 4LR11, an austenitic stainless steel with 18.4% Cr and 8.8% Ni.

5. Results

The stainless steel sample was put under a cyclic stress with a load amplitude of 18 kN and a frequency of 30 Hz. The results are presented in Figs. 6 and 7. Fig. 6 shows two

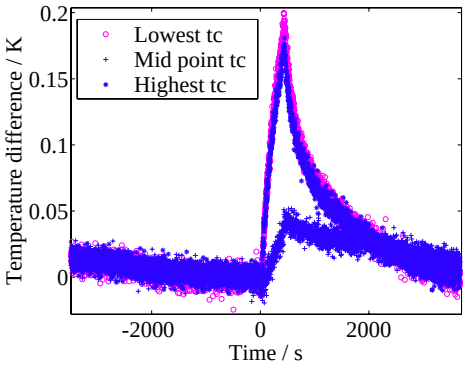

Fig. 6. Stainless steel, Sandvik 4LR11, an austenitic stainless steel with 18.4% Cr and 8.8% Ni, 4–22 kN, 30 Hz.

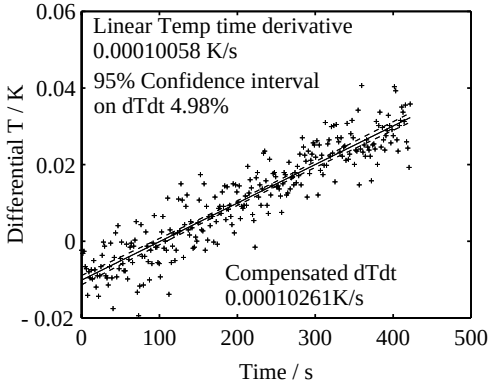

Fig. 7. Linear fit of the stainless steel data from the lower curve in Fig. 6 with an error estimate.

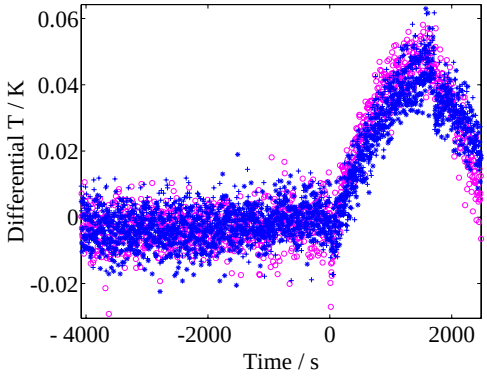

Fig. 8. Al, Swedish standard SS4253, sandcast with 10% Si and 0.3% Mg, 35 Hz, 0.4–4.3 kN Temperature–time plot from Matlab analysis.

curves. What appears to be the upper curve are the two overlapping curves representing the thermocouple readings for the two ends of the rod. The temperatures at the ends of the bar rise more rapidly. This disturbance has been discussed earlier and does not interfere with the mid point temperature of the bar during the time of the experiments used for evaluation of the heating rate.

Fig. 7 shows that the temperature increase is almost linear. The exponential fit was changed to a linear fit for numerical reasons. The calculated heating rate is shown in the upper left-hand corner. To compensate for the heating rate in the rod before commencing the cyclic loading, a compensated value is given in the lower right-hand corner of Fig. 7. The temperature–time derivative is approximately 10×10^{-5} °C/s.

The experiments with the aluminium alloy were carried out using three differential thermocouples. The sample was subjected to cyclic stress with a load amplitude of 3.9 kN and a frequency of 35 Hz. Fig. 8 shows how the temperature change from unloaded to cyclically loaded. A sudden change in the temperature–time curves is observed at this moment.

In Fig. 9, the temperature data from the sensor in the middle of the bar is fitted with an exponential function. The derivative of the temperature–time curve at the start of loading was calculated. The derivative is presented in

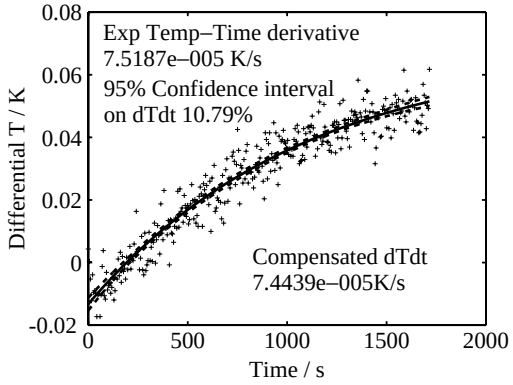

Fig. 9. Exponential fit to data in Fig. 8 for the Al alloy with error estimate.

Table 1
Thermophysical data for the tested materials

	Al	Stainless steel	Unit
c_p	900	500	J/K kg
ρ	2700	7900	kg/m^3
E	61×10^9	196×10^9	N/m^2
A	250×10^{-6}	250×10^{-6}	m^2
F	3900	18000	N
f	35	30	s^{-1}
dT/dt	7.44×10^{-5}	10×10^{-5}	K/s
η	4.12×10^{-4}	1.63×10^{-4}	

c_p is the thermal heat capacity, ρ the density, E the modulus of elasticity, A the cross-sectional area, F the force amplitude in compression, f the frequency, dT/dt the temperature derivative and η the loss factor.

the upper left-hand corner of Fig. 9. The statistical error of the derivative is calculated from the error of the parameters in the exponential fit. The slope of the temperature–time curve prior to the start is subtracted from the calculated derivative and the resulting value is stated in the lower part of Fig. 9. In this case, the derivative is 7.44×10^{-5} K/s. Although the temperature–time derivatives are similar for the two materials, the load input and material data for these two materials are quite different.

The thermophysical and geometrical data used in the evaluation is given in Table 1. The intrinsic material damping in the bottom row is calculated using Eq. (8).

6. Discussion

A comparison of the calculated data for the loss factor shows that the Al alloy has about 2.5 times better intrinsic material damping than the stainless steel. It is interesting to note that this is close to the inverse value of E^{Al}/E^{Fe}. It can be suggested that for a single-phase material, the material damping is highly dependent on the modulus of elasticity. It is reasonable to say that a higher modulus of elasticity decreases its material damping for single-phase materials. This will be further discussed in the next paper where there is a careful comparison between different materials.

7. Conclusion

A new method based on differential thermal analysis during cyclic loading has been developed. The initial tests of this method have shown that it is possible to measure small rates of temperature increase due to the internal conversion from mechanical energy to heat. This rate, together with the thermal capacity of the material makes it possible to calculate the amount of energy that is transferred to heat per unit of time, since the energy loss to the surroundings is small. This energy, divided by the measured input of mechanical energy per unit time gives a calculated value for the intrinsic material damping of the material.

After final statistical evaluation of the test data, a systematic evaluation of the effect of the material's internal structure on its intrinsic damping is planned.

Acknowledgements

This work has been made possible by a donation by Scania AB and the support of the Division of Casting, Royal Institute of Technology, KTH, Sweden for which we are most grateful. We wish to thank Scania AB for its financial support and aspecially Mr. Stenfors and Mr. Klopotek at Scania for their support and fruitful discussions. We would also like to thank Laboratoire de Thermodynamique et Physicochemie Metallurgiques at L'Institut National Polytechnique de Grenoble, especially Professor Michel Allibert for his kind support.

References

[1] V.K. Kinra, C.L. Yapura, A fundamental connection between intrinsic material damping and structural damping, Mechanics and Mechanisms of Material Damping, ASTM STP 1169 (1992) 396 (Philadelphia).
[2] A.D. Nashif, D.I.G. Jones, J.P. Henderson, Vibration Damping, Wiley, New York, 1985.
[3] A.A. Usoltsev, Damping capacity of vermicular graphite cast iron, Steel in the USSR, vol. 20, 1990.
[4] P.W. Spence, C.J. Kenchington, The Role of Damping in Finite Element Analysis, NAFEMS, 1993.
[5] D.J. Ewins, Modal Testing: Theory and Practice, Research Studies Press, England, 1984.
[6] Nowick and Berry, Anelastic Relaxation in Crystalline Solids, Academic Press, New York, 1972.
[7] J. Åberg, B. Widell, P. Larsson, Damping measurements on twelve metallic plates using frequency response measurements and a single degree of freedom circular fit analysis method, Eur. J. Phys., Experimental Techniques, (U.S.A.), submitted for publication.
[8] V.K. Kinra, G.G. Wren, Axial damping in metal-matrix composites. A new technique for measuring phase difference to 10exp-4 radians, Exp. Mech. (U.S.A.) 32 (1992) 163.
[9] G.G. Wren, V.K. Kinra, Axial damping in metal-matrix composites. Part II. A theoretical model and its experimental verification, Exp. Mech. (U.S.A.) 32 (1992) 172.
[10] J. Åberg, B. Widell, Uniaxial material damping using a fibre optic lattice—a discussion of its performance envelop, Exp. Mech. (U.S.A.), Accepted for publication.
[11] MTS Systems Corporation, http://www.mts.com.
[12] G.W. Burns, Temperature-electromotive force reference functions and tables for the letter-designated thermocouple types based on the ITS-90, NIST Monograph 175, National Institute of Standards and Technology, 1993.
[13] http://www.pentronic.com.
[14] http://www.electrolube.com.
[15] http://www.agilent.com, formerly named Hewlet-Packard Test and Measurement.
[16] C.M. Harris, C.E. Crede, Shock and Vibration Handbook, second ed., McGraw-Hill, New York, 1976.
[17] A. Wolfenden, V.K. Kinra, in: Proceedings of the 3rd International Symposium on M3D: Mechanics and Mechanisms of Damping, Norfolk, VA, USA, 1995, ASTM Special Technical Publication 1304.
[18] http://www.mathworks.com, Supplier of Matlab.